Published in final edited form as:
J Neurosci. 2010 December 15; 30(50): 16796–16808. doi:10.1523/JNEUROSCI.1869-10.2010.

The largest group of superficial neocortical GABAergic interneurons expresses ionotropic serotonin receptors

SooHyun Lee[1,2,3,*], **Jens Hjerling-Leffler**[1,3,*], **Edward Zagha**[1,2], **Gord Fishell**[1,3], and **Bernardo Rudy**[1,2]

[1]Smilow Neuroscience Program, Smilow Center, New York University School of Medicine, 522 First Avenue, New York, NY, 10016, USA

[2]Departments of Physiology and Neuroscience and Biochemistry, Smilow Center, New York University School of Medicine, 522 First Avenue, New York, NY, 10016, USA

[3]Department of Cell Biology, Smilow Center, New York University School of Medicine, 522 First Avenue, New York, NY, 10016, USA

Abstract

A highly diverse population of neocortical GABAergic (gamma-aminobutyric acid) inhibitory interneurons has been implicated in multiple functions in information processing within cortical circuits. The diversity of cortical interneurons is determined during development and largely depends on their embryonic origins either from the medial (MGE) or the caudal (CGE) ganglionic eminences. While MGE-derived parvalbumin- (PV) or somatostatin- (SST) expressing interneurons are well characterized, less is known about the other types of cortical GABAergic interneurons, especially those of CGE lineage, due to the lack of specific neuronal markers for these interneuron subtypes. Using a bacterial artificial chromosome (BAC) transgenic mouse line, we showed that, in the somatosensory cortex of the mouse, serotonin 5HT3a (5-hydroxytryptamine 3a) receptor, the only ionotropic serotonergic receptor, is expressed in most, if not all, neocortical GABAergic interneurons that do not express PV or SST. Genetic fate mapping and neurochemical profile demonstrate that 5HT3aR-expressing neurons include the entire spectrum of CGE-derived interneurons. We report that in addition to serotonergic responsiveness via 5HT3aRs, acetylcholine (ACh) also depolarizes 5HT3aR-expressing neurons via nicotinic receptors. 5HT3aR-expressing neurons in thalamocortical (TC) recipient areas receive weak but direct monosynaptic inputs from the thalamus. TC input depolarizes a subset of TC-recipient 5HT3aR neurons as strongly as FS cells, in part due to their high input resistance. Hence, fast modulation of serotonergic and cholinergic transmission may influence cortical activity through an enhancement of GABAergic synaptic transmission from 5HT3aR-expressing neurons during sensory process depending on different behavioral states.

Keywords

GABAergic interneuron; cortex; serotonergic; cholinergic; development; thalamocortical

Introduction

Neuromodulator systems provide a mechanism by which small groups of neurons in subcortical nuclei can broadly influence cortical activity. Conversely, disruption of such

Correspondence should be addressed to Bernardo Rudy. Phone: 212-263-0431 Bernardo.Rudy@nyumc.org.
*these two authors contributed equally to this manuscript.

modulation, may impair various physiological processes, and can potentially lead to neurological disorders (Freund, 2003; Lewis and Hashimoto, 2007). The profound influence of these neuromodulators on the cortex, likely in part stems from their preferential targeting of inhibitory cortical interneurons releasing GABA (Beaulieu and Somogyi, 1991; Smiley and Goldman-Rakic, 1996). Cortical GABAergic interneurons play critical roles in controlling activity through feedforward and feedback inhibition (Freund and Buzsáki, 1996; McBain and Fisahn, 2001; Freund, 2003; Buzsáki et al., 2004), and are heterogeneous with regards to their developmental origin, expression of neurochemical markers, electrophysiological properties, morphology, and cellular and subcellular location of output synaptic contacts (Ascoli et al., 2008). Understanding cortical interneuron diversity is critical to understanding the emergence and function of cortical networks.

Here we focused on cortical interneurons that express the 5-hydroxytryptamine (serotonin) receptor 3a (5HT3aR), which is the only known murine serotonergic ionotropic receptor (Barnes and Sharp, 1999; Chameau and Van Hooft, 2006). In the mature neocortex the 5HT3aR is present exclusively in GABAergic interneurons (Morales and Bloom, 1997; Chameau and van Hooft 2006), including VIP and/or CCK positive bipolar cells and multipolar neuropeptide Y (NPY)-expressing cells (Férézou et al., 2002; Inta et al., 2008; Varga et al., 2009; Vucurovic et al., 2010). However, the full extent of the expression of the 5HT3aR in cortical interneurons and the representation of 5HT3aR-expressing interneurons of the total interneuron population are unknown. This knowledge is critical to understand the function of fast serotonergic signaling in cortex. By taking advantage of *5HT3aR-BAC*^{EGFP} transgenic mice, we have undertaken a systematic approach to understanding the population of 5HT3aR-expressing interneurons in somatosensory cortex. We find that the population of 5HT3aR-expressing interneurons is large, particularly in supragranular layers, where it represents the major interneuron population. In fact, nearly all interneurons that do not express PV or SST are 5HT3aR-expressing. Thus, most, if not all, cortical interneurons can be assigned to one of three groups PV-, SST- or 5HT3aR-expressing interneurons.

While PV and SST are derived from the MGE, the CGE is the origin of most interneurons that do not express these markers (Nery et al., 2002; Xu et al., 2004; Butt et al., 2005; Cobos et al., 2006; Miyoshi et al., 2010). This includes the reelin-expressing late-spiking neurogliaform cells as well as bipolar/bitufted VIP-expressing cells. Using genetic fate mapping we directly show the CGE-origin of a majority of 5HT3a-expressing neurons and exclude the MGE as a source. Accordingly, we find the same anatomical and electrophysiological subtypes as those described in the CGE-derived population. Although heterogeneous, the 5HT3aR-expressing populations uniformly respond to serotonergic and cholinergic modulation. In addition, a subpopulation of these interneurons receives weak thalamocortical inputs whose influence on cortical networks might be functionally gated by their serotonergic input. Thus, 5HT3aR-expressing interneurons are uniquely posed to influence cortical sensory processes through their ability to convey fast effects of convergent long-range cortical afferents.

Material and Methods

In vivo fate mapping

In order to perform genetic fate mapping of the CGE and MGE respectively, male mouse mutants for *Mash1-BAC*^{CreER} (heterozygous or homozygous) (Battiste et al., 2007) or *Nkx2-1-BAC*^{Cre} (heterozygous) (Xu et al., 2008) on a *R26R*^{tdRFP} (homozygous) background (Luche et al., 2007) was crossed to *5HT3aR-BAC*^{EGFP} (heterozygous) females. In the case of inducible genetic fate mapping using the *Mash1-BAC*^{CreER} four milligrams of tamoxifen was administered orally between noon to 2 pm at E12.5, E14.5 and E16.5.

Tissue preparation for immunocytochemistry and *in situ* hybridization

For *in situ* postnatal brains were fixed by transcardiac perfusion followed by 1 hour postfixation with 4% PFA on ice. Embryonic brains where dissected and then fixed over night in 4% PFA at 4°C. Brain tissue was cryoprotected using a 15% followed by 30% sucrose/PBS solution overnight at 4°C. Tissues were embedded in Tissue Tek, frozen on dry ice, and sectioned at 20 μm. For immunohistochemistry mice were fixed by transcardiac perfusion with 0.9% saline containing heparin (1 U/mL), followed by 30-50 mL of 0.1 M phosphate buffer (PB; pH 7.4) containing 4% paraformaldehyde. Dissected brains were further fixed in the same fixative solution for one hour at 4°C and then placed in a 30% sucrose solution at 4°C for 24 hours. Using a sliding microtome, 40 μm thick frozen coronal sections were collected in 0.1 M phosphate-buffered saline (PBS).

Immunohistochemistry

Sections were washed in PBS and then incubated in a blocking solution (10% normal goat serum, 1% BSA, 0.2% cold fish gelatin, and 0.2% Triton X-100 in PBS) for one hour at room temperature. Sections were then incubated in primary antibodies in a diluted (1:10) blocking solution overnight at 4°C, washed in PBS 4 × 5 min and 1 hour of secondary antibody incubation at room temperature, followed by 4 × 5 min PBS washes. Nuclear counterstaining was performed with 100 ng/ml 4,6-diamidino-2-phenylindole (DAPI) solution in water for 10 min. Primary antibodies were used in the following concentrations: mouse anti-Parvalbumin (1:1000, Sigma), rat anti-somatostatin (1:500, Chemicon), rabbit anti-somatostatin (1:1000, Chemicon), rat anti-platelet-derived growth factor receptor (PDGFR; 1:500, BD PharMingen), rabbit anti-Neuropeptide Y (1:500, Incstar), sheep anti-Neuropeptide Y (1:500, Abcam), rabbit anti-Vasoactive intestinal polypeptide (1:500, Incstar), rabbit anti-Calretinin (1;1000, Chemicon), mouse anti-Calretinin (1:1000, Chemicon), mouse anti-Reelin(1:500, MBL), mouse anti-cholecystokinin (1:1500, Sigma), rabbit anti-SatB2 (1:1000, Abcam), rat anti-EGFP (1:2000 Nacalai Tesque) and rabbit anti-Olig2 (1:1000, Chemicon). Secondary antibodies conjugated with Cy3, and Cy5 (1:200, Jackson ImmunoResearch) or Alexa fluoro dyes 488 and 594 (1:1000 Molecular Probes) were used to visualize the signals. Fluorescent images for cell counting were taken using a Zeiss LSM 510 META confocal microscope (Thornwood, NY).

Double *In Situ* Hybridization

Sections were dried for 1 hour before 10 minute fixation in 4% PFA. After wash endogenous peroxidase activity was quenched by 1.5% H_2O_2 in Methanol for 15 at room temperature. Sections were then treated in 0.2M HCl for 8 minutes before a Proteinase K treatment (10ug/ml; Roche) for 3 minutes and a post-fixation in 4% PFA 10 minutes at 4°C with washing steps in between. Before hybridization the tissue was acetylated in TEA (0.185 g/ml; Sigma Aldrich), 0.5N NaOH and 0.25% Acetic Anhydride (Sigma-Aldrich). The DIG and FITC labeled probes (full length cDNA probes of *Gad67*, *PV*, *SST*, *EGFP* and *5HT3aR*) were mixed 2 μl per slide in 250 μl hybridization buffer (50% formamide, 10% Dextrane Sulfate, 0.25 mg/ml yeast RNA, 0.3M NaCl, 20mM Tris, 5mM EDTA, 10mM NaPO4 and 1% n-Lauroylsarcosine in Denhardt's solution) and denatured at 80°C for 2 minutes. Hybridization was made overnight at 55°C. After hybridization the sections was rinsed in a 2x SSC with 50% Formamide solution for 30 minutes at 65°C before several washes in RNAse buffer (0.5M NaCl, 10mM Tris pH 7.5 and 5mM EDTA pH 8.0). The tissue was treated with RNAse (20 μg/ml; Roche) in RNAse buffer for 30 minutes at 37°C before rinsing in decreasing amounts of SSC (2x, 0.2x and 0.1x) for 15 minutes at 37°C each. After equilibrating in TN buffer (0.1M Tris pH7.5 and 0.15M NaCl) the sections were blocked in 0.5% blocking reagent (Roche) in TN buffer for 30 minutes at room temperature. The sections were then incubated with primary antibody against FITC or DIG (which ever is the weakest probe) over night at 4°C. On the third day sections were rinsed in TNT buffer (TN

buffer with 0.05% Tween*20) before amplification and visualization step using the TSA Plus Cyanine 3/Fluorescein System (Perkin Elmer) according to manufacture's instruction (10-60 minutes incubation). After washes in TNT the peroxidase was quenched in 3% H_2O_2 in TN for 2 hours at room temperature before incubation with the other primary antibody for 1 hour at room temperature followed by visualization using the same kit as above. After washes in TNT sections were incubated in DAPI before mounting in Fluoromount-G. Images were obtained by fluorescent microscopy on a Zeiss Axioskop using Spot Advanced software and/or by confocal microscopy using a Zeiss LSM 510 Meta system (Thornwood, NY, US).

Slice preparation for electrophysiology

All procedures were conducted in accordance with the NIH Guide for the Care and Use of Laboratory Animals. The *5HT3aR-BAC*^{EGFP} transgenic mouse line was provided by GENSAT. Mice (14-21 days old) were anesthetized with intraperitoneal injection of pentobarbital (100 mg/kg body weight) and decapitated. The brain was quickly removed and immersed in ice-cold oxygenated artificial cerebrospinal fluid (ACSF) containing (in mM) 125 NaCl, 26 $NaHCO_3$, 2.5 KCl, 1.25 NaH_2PO_4, 2 $CaCl_2$, 2, $MgCl_2$, and 10 glucose. Coronal slices (300 μM) were made using Vibratome 1000 Plus (Vibratome, St. Louis, MO), incubated at room temperature in ACSF for an hour prior to recording. For thalamocortical recording, TC slices (400 μm) were prepared from mice aged postnatal day 14 -17, as previously described (Agmon and Connors 1991, Kruglikov and Rudy, 2008). The ACSF solution was continuously equilibrated with 95% O_2 and 5% CO_2 throughout cutting, slice incubation, and recording.

Electrophysiological recordings

Whole cell current-clamp recordings were performed using micropipettes (3-6 MΩ) filled with internal solution containing (in mM) 135 K-gluconate, 4 KCl, 2 NaCl, 10 HEPES, 0.2 EGTA, 4 ATP-Mg, 0.3 GTP-Tris, 1,4 phosphocreatine-Tris (pH 7.25, 280 mOsm) and biocytin. Membrane potentials reported here were not corrected for the liquid junction potential. Recordings were conducted at 29 - 32°C. When patching, cell-attached seal resistances were >1 GΩ and series resistance after achieving whole cell configuration was between 5 and 25 MΩ. A series of hyperpolarizing and depolarizing step currents were injected to measure intrinsic properties of each neuron. Data were collected using an Axopatch 200B amplifier (Molecular Devices, Union City, CA), lowpass filtered at 5 kHz, digitized at 16-bit resolution (Digidata 1322A; Axon Instruments) and sampled at 20 kHz. pCLAMP 9 software (Axon Instruments) was used for data acquisition, and analysis was performed using the Clampfit module of pCLAMP. For TC recording, bipolar stimulating electrodes were placed at the border of the VB and brief current pulses (20Hz) with increasing intensity was delivered while performing simultaneous whole-cell recordings from neurons in deep L3 and L4 of barrel cortex. To visualize the recorded neurons, slices were fixed for overnight with 4% paraformaldehyde in PBS, rinsed with PBS, and incubated in a blocking solution (1% normal goat serum and 0.3% TritonX-100 pH7.5 in PBS) for 2 hours. After several washes with PBS, Biocytin-filled neurons were stained using streptavidin conjugated Alex Flour 555 (1:500 dilution, Invitrogen). Fluorescently labeled neurons were imaged and reconstructed using a Zeiss LSM 510 META confocal microscope (Thornwood, NY, US) and Neurolucida software (Microbrightfield, Williston, VT, US).

Electrophysiological analysis

To characterize the intrinsic membrane properties of neurons, hyper- and depolarizing current steps of 500 ms duration were applied in 1-20 pA increments at 0.2 Hz as described previously (Miyoshi et al., 2010). The following parameters were measured. RMP (mV): resting membrane potential, the stable membrane potential reached a few minutes after

breaking the membrane with no holding current applied. R_m (MΩ): input resistance, the slope of the regression line fitted to the I-V curve (usually between -50 and -10 pA), as measured at the end of the 500-ms voltage responses. Tau (ms): membrane time constant, determined from the monoexponential curve best fitting to the average voltage response to hyperpolarizing current steps of -40 to -20 pA using fitting fuction in Clampfit 9 (Axon instruments). Delay to spike (ms): time to first spike from the beginning of current injection. Spike threshold (mV): the membrane potential at the point at which the interpolated rate of voltage rise (dV/dt) reached >10 mV/1 ms. Spike height (mV): action potential amplitude, measured from the threshold to the peak. Spike width (ms): action potential duration, the spike width at its half amplitude. AHP (mV): peak amplitude of the afterhyperpolarization (AHP), measured from the spike threshold. tAHP (in ms): AHP latency, the time interval between spike threshold and the hyperpolarization nadir. Maximum firing frequency (Hz): spike frequency in response to 20 times of rheobase current step. Adaptation: frequency adaptation, percentage of decrease in the frequency from first 100ms to last 100ms.

Results

Interneuron specific expression of 5HT3aR in the mouse cortex

We used a mouse-line expressing EGFP under the control of the 5*Htr3aR*-promoter (5*HT3aR-BAC*^{EGFP}) provided by the GENSAT project at Rockefeller University. In order to assess whether 5*HT3aR-BAC*^{EGFP} driven EGFP-expression reflects true *Htr3a*-gene transcription we performed double in situ hybridization for *EGFP* and *5HT3aR* mRNA. We found near complete overlap between the *EGFP* and the 5*HT3aR* signals indicating that EGFP expression is indeed specific to cells expressing 5HT3aRs and that virtually all 5HT3aR-expressing neurons express EGFP (99.8 ± 0.3%) (Fig. 1*A*). We also performed double in situ hybridization for *EGFP* and *Gad67*. All cells that expressed *EGFP* also expressed *Gad67* mRNA indicating that at the age tested (p21) 5HT3aR expression is confined to a GABAergic population (Fig. 1*B*). This conclusion was further strengthened by the complete lack of overlap between EGFP and the pyramidal cell marker Satb2 or the oligodendrocyte marker Olig2 by immunohistochemistry (Fig. 1*C*,*D*) (Lu et al., 2000;Zhou and Anderson, 2002;Britanova et al., 2008).

5HT3aR-expressing neurons constitute the third major group of interneurons and are densely present in superficial layers

Previous studies have shown that interneurons expressing the 5HT3aR include neurons containing VIP, calretinin (CR) and neuropeptide Y (NPY) but not parvalbumin (PV) or somatostatin (SST) (Férézou et al., 2002; Inta et al., 2008; Vucurovic et al., 2010). Consistent with this, we detect no, or nearly no, overlap between PV- or SST- and GFP-expression in the 5*HT3aR-BAC*^{EGFP} mouse respectively (Fig. 4). In order to elucidate the population of 5HT3aR-expressing neurons and determine its contribution to the total interneuron population, we used double in situ hybridization to determine the proportion and layer distribution of Gad67-expressing neurons that express 5HT3aR and compared this to the PV- and SST-expressing populations. We also performed double ISH for PV and SST to determine the overlap of the mRNA of these two markers (Fig. 2*A*-*C*, quantified in *D*). We first analyzed the laminar distribution of 5HT3aR-expressing neurons (Fig. 2*D*), and found that more than two thirds of these cells have cell bodies positioned within superficial layers of Gad67-expressing neurons (L1 15 ± 0.3% and L2/3 54 ± 0.6%). Within layers 1, and 2/3, the number of 5HT3aR-expressing neurons exceeds the number of PV positive neurons by more than two fold, indicating that the major type of GABAergic interneuron in superficial layers of the cortex is the 5HT3aR-expressing population. Furthermore, by combining the results from the four different *in situ* hybridizations we find that with the possible exception of ~5% of neurons in layer I, we can ascribe every GABAergic neuron in somatosensory

neocortex to one out of three groups expressing PV, SST or 5HT3aR. The deviation from 100% in Fig 2*D* was caused by the cumulative variation resulting from combining the four different double *in situ* hybridization experiments. We conclude that the 5HT3aR expressing cells not only primarily populate superficial layers, but are in fact the most predominant population of interneurons within this region. More importantly, collectively PV, SST or 5HT3aR labeling account for nearly 100% of all GABAergic interneurons.

A majority of 5HT3aR-expressing cells are derived from the caudal ganglionic eminence

Given the *5HT3aR-BAC*^{EGFP} expression was restricted to non-PV/SST interneurons in mature animals, we set out to determine the site(s) of origin of this population. Cortical interneurons are mainly derived from two different ventral progenitor zones, the caudal and medial ganglionic eminences (CGE and MGE respectively) (Anderson et al, 1997a, 1997b; Wichterle et al., 1999; Wichterle et al., 2001; Nery et al., 2002; Butt et al., 2005). *5Htr3aR-BAC*^{EGFP} animals examined at all embryonic time points (beginning at embryonic day (E) 12) had EGFP expression within the CGE but not in the MGE/LGE (Fig. 3*A*,*B*). Furthermore, there was an extension of the expression into the stria terminalis and the pre-optic area (POA), a region that has been shown to give rise to a small subset of cortical interneurons (Gelman et al., 2009). *In situ* hybridization analysis for *5HT3aR* at these time points yielded similar results (Fig. 3*C*). In agreement with previous findings, we also observed extensive EGFP-expression by preplate neurons including Cajal-Retzius cells (Fig. 3*A*,*B*) (Inta et al., 2008; Chameau et al., 2009). Since the expression of the 5HT3aR may be dynamic, we set out to investigate whether the cells expressing 5HT3aR embryonically are the same cells expressing it in the adult. To this end we utilized two different genetic fate-mapping strategies (Xu et al., 2008; Miyoshi et al., 2010) to investigate from which zone the cortical EGFP-labeled cells were derived. Using the *Nkx2.1-BAC*^{Cre} mouse together with the red *R26R*^{tdRFP} reporter mouse (Luche et al., 2007) we labeled cells originating from the MGE. When these mice were crossed onto the *5HT3aR-BAC*^{EGFP} mice we saw no overlap between EGFP and tdRFP-expression, indicating that the 5HT3aR-expressing cells in mature cortex are not derived from the MGE (Fig. 3*E*, quantified in 3*G*). We have recently shown that one can efficiently label cells derived from the CGE using a *Mash1-BAC*^{CreER} mouse to direct the tamoxifen-induced cre-recombination of a reporter line (Miyoshi et al., 2010). We used the *Mash1-BAC*^{CreER}; mouse together with the *R26R*^{tdRFP} reporter to confirm that 5HT3aR-expressing neurons originate from the CGE. Although neuronal labeling was most prominent, we observed some tdRFP-expression within oligodendrocytes. The immunohistochemical marker CC1 was used to exclude these cells from the analysis (Bhat et al., 1996). We observed a 91 ± 1% overlap between interneurons derived from a tamoxifen induced E16.5 labeling of the *Mash1-BAC*^{CreER}*;R26R*^{tdRFP} and the *5HT3aR-BAC*^{EGFP} driven EGFP expression, showing that 5HT3a-expressing cells are derived from the CGE and not from the MGE (Fig. 3*F*, quantified in 3*H*). This was also true at earlier gavage points (data not shown).

Neurochemical profile of 5HT3aR-expressing neurons

According to our ISH analysis 5HT3aR interneurons compromise 28.8 ± 2.2% of the neurons in somatsensory cortex that express the pan-GABAergic marker Gad67. To parse out the 5HT3aR population in this region in more detail, we analyzed their expression of a variety of neurochemical interneuron markers (Ascoli et al., 2008). Although some molecular markers may not precisely correlate with different interneuron subtypes, their expression does provide a strong indicator of their anatomical and electrophysiological properties. We used as markers two calcium-binding proteins (PV and CR), and four neuropeptides (SST, CCK, VIP and NPY), all which are exclusively expressed in GABAergic interneurons in neocortex (Fig. 4*A*-*F*). In addition to these six markers, we also examined the expression of Reelin, which was recently reported as a marker of GABAergic

neurons (Miyoshi et al., 2010). Reelin is expressed in subpopulations of both MGE- and CGE-derived interneurons but all MGE-derived Reelin positive cells appear to also express SST, suggesting that all Reelin+/SST- cells are CGE-derived. To accurately estimate the proportion of all 5HT3aR-expressing neurons expressing these seven neuronal markers, we also examined the degree of overlap of many of these markers in 5HT3aR-expressing neurons, using double immunohistochemical analysis (Fig. 4*E*,*F*). With these markers, we were able to account for more than 85% of the 5HT3aR-expressing neurons in the primary somatosensory cortex (Fig. 4*E*).

In agreement with previous findings and consistent with our in situ results, we never observed colocalization of PV with 5HT3aR positive neurons (Férézou et al., 2002; Inta et al., 2008; Vucurovic et al., 2010). Moreover, less than 3% of 5HT3aR-expressing neurons were found to express SST (Fig. 4*E*). The finding that 5HT3aR-expressing neurons do not express these MGE-derived interneuron markers is also consistent with the results from the fate-mapping (Fig. 3*E*). Notably, nearly all VIP and or CCK positive neurons expressed 5HT3aR as well as a majority of NPY-expressing cells (Fig 4*C*). NPY is reportedly found in SST- (Wonders and Anderson, 2006) as well as in PV-expressing populations (Karagiannis et al., 2009). This result is consistent with previous findings that 5HT3aR was detected in GABAergic interneurons coexpressing CCK and VIP in both cortex and hippocampus (Morales and Bloom 1997; Férézou et al., 2002; Vucurovic et al., 2010). We find that reelin and CR partially overlap with SST (Pesold et al., 1999; Miyoshi et al., 2010) and therefore only a fraction of the reelin and CR populations expressed 5HT3aR (Fig. 4*B*,*C*). We also analyzed the layer distribution of these markers within the 5HT3aR-expressing population (Fig. 4*C*,*D*,*F*). Reelin was expressed by a large majority (73.0 ± 4.0%) of 5HT3aR-expressing neurons in L1 (Fig. 4 *D*). The proportion 5HT3aR cells expressing NPY was highest in deeper layers (40 ± 7.5% of EGFP positive cells in L4 and 40 ± 3.5% in L5/6) (Fig. 4*D*). Conversely, in layers 2/3 and 4 most NPY cells are 5HT3aR positive (82 ± 4% and 92 ± 8.5% respectively) while only about 60% of NPY cells in layer 5/6 express the 5HT3aR (Fig. 4*C*).

Intrinsic physiological properties of 5HT3aR-expressing neurons

To examine the electrophysiological and morphological profile of 5HT3aR-expressing neurons, we performed whole-cell recordings from EGFP-expressing neurons (n = 132) in superficial layers of the primary somatosensory cortex using an acute slice preparation (Fig. 5). Cells were recorded in current clamp and 500 ms hyper- and depolarizating steps were used to assess their intrinsic membrane properties, while biocytin was added in the recording pipette to allow for post-hoc morphological analysis. Based on these intrinsic membrane properties, as well as morphology, we classified the 5HT3aR-expressing neurons according to previously described criteria (Miyoshi et al., 2010). Miyoshi et al. (2010) described nine different types of CGE-derived interneurons, here we observed all except two of the rarest types (delayed intrinsic bursting, dIB and sigmoid intrinsic bursting, sIB). This included two different late-spiking subtypes (LS1; 34.6%, LS2; 11.3%) (Kawaguchi, 1995;Chu et al., 2003;Tamás et al., 2003;Miyoshi et al., 2007;Oláh et al., 2007), bipolar/bitufted irregular spiking cells (IS, 22.5%) (Cauli et al., 1997;Porter et al., 1998;Cauli et al., 2000;Galarreta et al., 2004), the “arcade axon” delayed non-fast spiking (dNFS3, 2.2%) (Butt et al., 2005;Kawaguchi and Kubota, 1996), the fast-adapting cells (fAD, 12.0%) (Butt et al., 2005), as well as burst non-adapting cells (bNA1; 13.5%, bNA2; 3.7%) (Kawaguchi and Kubota, 1996;Kawaguchi and Kubota, 1997;Butt et al., 2005;Caputi et al., 2009;Rozov et al., 2001).

Late-spiking cells, LS1 and LS2, were characterized by a long delay with a steady ramp depolarization leading up to the initial spike at threshold current injections. Miyoshi et al., (2010) showed that both of these types express reelin but have significantly different electrophysiological and morphological properties. Electrophysiologically, LS1 is

distinguished from LS2 in that the delay persists even when up to 3-5 spikes are induced during just supra-threshold current injection steps, while LS2 cells never show a pronounced delay when more than one spike is elicited. Both cell types showed firing frequency adaptation and non-monotonic spike amplitude accommodation. LS1 possess a small soma and have locally ramifying short thin dendrites and a dense local axonal plexus. Thus, their morphology is similar to previously described cortical neurogliaform cells (Kawaguchi, 1995; Tamás et al., 2003; Miyoshi et al., 2007, Oláh et al., 2007). Similar to the description in Miyoshi et al. (2010) we found that LS2 neurons had lower input resistance and maximum firing rate compared to LS1 cells (Table 1), and larger soma size and thicker, longer, but less branching dendrites. IS neurons showed irregular firing patterns during intermediate current steps and strong monotonic spike amplitude accommodation throughout supra-threshold current injections. Most IS neurons exhibited a bipolar / tripolar morphology and had axonal trees projecting towards deeper layers. 5HT3aR-expressing interneurons with an IS firing pattern resembled those previously described as VIP- and CR-positive bipolar interneurons (Cauli et al., 1997; Porter et al., 1998; Cauli et al., 2000; Galarreta et al., 2004, Miyoshi et al., 2010). Interestingly, we observed an irregular-spiking multipolar cell that was not described in the Miyoshi et al (2010) study (Fig. 5). This subtype appeared very similar to those cells described as derived from the Nkx5-1^{Cre} labeled population from the POA (Gelman et al., 2009). Fast adapting cells (fAD) are characterized by their failure to fire throughout the 500 ms step during supra-threshold depolarization. This subtype has been suggested to be the largest VIP-positive CR-negative population (Porter et al., 1998; Miyoshi et al., 2010). The last major subtype we identified was the burst non-adapting (bNA1) subtype that exhibited bursts of two or three spikes, followed by regular spiking. The bNA1 cells have a distinct feature giving rise to a “hump” at the beginning of the 500 ms current injection during near-threshold steps.

In addition to the six subtypes described above (accounting for 94% of all 5HTR3aR cells), we identified a second bursting non-adapting subtype (bNA2) with intrinsic properties and morphology similar to previously described CR and VIP expressing bipolar shaped interneurons (Kawaguchi and Kubota, 1996; Cauli et al., 1997; Rozov et al., 2001; Butt et al., 2005; Caputi et al., 2009). We also identified a small bipolar dNFS3 subtype that exhibits an “axon arcade” morphology, which has been reported to be VIP-positive (Kawaguchi and Kubota, 1996). These results both confirm and extend our previous analysis and suggest that 5HT3R neurons include both CGE (the large majority) and most likely the POA populations.

Functional expression of 5HT3aRs

In the transgenic mouse line used in this study, expression of EGFP is driven by regulatory elements of the *Htr3a* gene. We have shown that the EGFP signal accurately predicts the expression of *5HT3aR* mRNA, as detected by *in situ* hybridization. In order to confirm that this signal corresponds to the presence of functional receptors, we tested the effect of mCPBG, a 5HT3aR selective agonist, on EGFP positive neurons (Fig. 6A). We applied mCPBG (100 μM) directly onto the soma of the recorded cell by puffing (30msec) through a second patch pipette located approximately 10 μm away from the soma. mCPBG application evoked fast depolarization, often leading to robust firing, in all EGFP-positive cells tested, including all layers (L1, n = 9; L2/3, n = 25; L4, n = 6; L5/6, n = 5) and all subtypes (LS1, n = 12; LS2, n = 6; IS, n = 10; bNA1, n = 11; bNA2, n = 2; fAD, n = 3; dNFS3, n = 1). Bath application of tropisetron (10nM), a 5HT3aR specific antagonist, completely blocked the response to mCPBG puffing. As a control, mCPBG was applied to PV- and SST-expressing neurons identified using the B13 (Chattopadhyaya et al., 2004;Dumitriu et al., 2007) and GIN (GFP-expressing inhibitory neuron) (Oliva et al. 2000,Fanselow et al., 2008) transgenic mouse lines, respectively. Neither FS (n = 3) nor SST (n = 3) neurons showed membrane

depolarization in response to mCPBG application directly onto the soma of the recorded neurons (Fig 6 *B,C*). These results demonstrate that EGFP-expressing neurons in the cortex of *5HT3aR-BAC*^{EGFP} mice express functional ionotropic serotonin receptors. It is important to note that careful application of the agonist is required because mCPBG desensitizes the 5HT3aR quickly and approximately 15 minutes are required for recovery after a previous puffing.

Single cell RT-PCR has shown that neurons that express 5HT3aRs in the cortex and hippocampus of the rat also express nicotinic acetylcholine receptors (Férézou et al., 2002). To confirm this we tested whether EGFP-positive neurons in L2/3 of the *5Htr3a-BAC*^{EGFP} mouse respond to cholinergic and nicotinic agonists. Brief application of the cholinergic agonist, carbachol (1mM, 30 ms puff) depolarized 5HT3aR-expressing neurons and evoked bursts of spikes (Fig. 6 *D1*). We further tested which cholinergic receptors are responsible for the depolarization of 5HT3aR-expressing neurons. Brief application of nicotine (100uM, 30ms puff) depolarized 5HT3aR-expressing neurons (Fig. 6 *D*2), while muscarine (100uM, 30ms puff) did not affect the membrane potential of the same neuron (Fig. 6 *D*3). All of the 5HT3aR-expressing cells tested, including cells in all layers (L1, n = 8; L2/3, n = 22; L4, n = 5; L5/6, n = 6) and of all subtypes (LS1, n = 10; LS2, n = 3; IS, n = 9; bNA1, n = 9; bNA2, n = 2; fAD, n = 6; dNFS3, n = 2) responded to nicotine application. Together, these data suggest that both serotonin and acetylcholine, can evoke fast synaptic activation of 5HT3aR-expressing neurons independently of layer and subtype.

Direct thalamocortical synaptic input to 5HT3aR-expressing neurons

Thalamocortical (TC) afferents directly contact both excitatory and inhibitory neurons in L4 and deep L3 in the cortex (Agmon and Connors, 1991; Swadlow and Gusev, 2000; Bruno and Simons, 2002; Wehr and Zador, 2003; Gabernet et al., 2005; Wilent and Contreras, 2005; Cruikshank et al., 2007; Hull et al., 2009, Cruikshank et al., 2010). Activation of both excitatory and inhibitory neurons establishes a simple disynaptic circuit that provides powerful, local feedforward inhibition due to stronger and faster TC excitation to FS interneurons than to excitatory neurons, which are mainly spiny stellate and star pyramidal neurons (Bruno and Simons, 2002; Swadlow, 2002; Gabernet et al., 2005; Cruikshank et al., 2007; Hull et al., 2009, Cruikshank et al., 2010). Agmon et al. (1991) has suggested that non-FS neurons are also recruited, but the nature of these cells has not been identified. Several lines of evidence suggest that the SST-expressing population is not recruited by TC stimulation (Beierlein et al., 2003; Cruikshank et al., 2010). We therefore examined whether TC afferents also directly recruit 5HT3aR interneurons (Fig. 7). We recorded from 5HT3aR-expressing neurons in deep L3 and L4 while delivering a brief extracellular stimulus to thalamic afferents with an electrode placed in fibers from ventrobasal (VB) nucleus of the thalamus in a TC slice preparation (Agmon and Connors, 1991). Evoked EPSCs in 5HT3aR-expressing neurons were recorded under voltage clamp recordings in which the post-synaptic soma was held at -70mV, while applying electrical stimulation to TC fibers at 20Hz. For comparison, we also recorded FS from neurons as identified by EGFP-expression in the B13 mouse. To elicit reliable responses, we adjusted the stimulation intensity to two fold higher than minimal stimulation intensity. An average latency of the evoked EPSCs in 5HT3aR-expressing neurons measured from the beginning of the stimulation artifact was 3.06 ± 0.35 ms. This is consistent with previous studies of monosynaptic thalamocortical EPSCs onto excitatory and FS neurons (Porter et al., 2001; Beierlein et al., 2003; Kruglikov and Rudy, 2008). EPSC latency of FS neurons (2.90 ± 0.18 ms) did not significantly differ from that on 5HT3aR-expressing neurons (p = 0.45). TC stimulation evoked significantly smaller EPSCs in 5HT3aR-expressing neurons than in FS (Fig. 7*B,F*, 38.06 ± 14.13 vs. 240.02 ± 85.59 pA, p = 0.0005). The synaptic response in a majority of TC recipient 5HT3aR-expressing neurons exhibited marked depression of the EPSCs evoked during a

train of 20 Hz TC stimulation (Fig. 7*G*, 11 out 15 neurons, EPSC2/EPSC1, 0.53 ± 0.14). A subset of 5HT3aR-expressing neurons, however, showed either no change or facilitation to repetitive thalamic stimulation (Fig. 7*G*, 4 out of 15 neurons, EPSC2/EPSC1, 1.24 ± 0.08). In contrast, all recorded FS neurons showed strong depression of thalamo-cortical EPSCs (EPSC2/EPSC1, 0.52 ± 0.13).

In a subset of recorded TC recipient 5HT3aR-expressing neurons we also measured the depolarization of the membrane potential evoked by thalamic stimulation under current-clamp recording configuration. On average, similarly to the EPSCs, smaller EPSPs were elicited on 5HT3aR-expressing neurons compared to those on FS (Fig. 7*H*, 2.88 ± 0.8 mV vs. 4.93 ± 0.75, p = 0.07), however the difference is only <2-fold compared to the 6-fold difference in EPSCs indicating that 5HT3aR cells are more responsive to small synaptic currents. Interestingly, in a subset of 5HT3aR-expressing neurons, TC stimulation evoked EPSPs comparable to those of FS neurons. As an example, TC stimulation evoked almost nine times smaller synaptic current in an LS1 type 5HT3aR neuron (Fig. 7 *A*1) than a FS neuron (Fig. 7 *B1, B2*; 58 pA and 508 pA respectively). Despite far less TC synaptic current to the 5HT3aR neuron, TC stimulation depolarized the LS1 neuron similar to the FS neuron (Fig. 7 *C1, C2*; 5.4 mV and 6.5 mV respectively). The input resistance of the LS1 neuron was three times higher than that of the FS neuron (302 MΩ and 98 MΩ respectively). It is likely that the much higher input resistance of 5HT3aR neurons is, in part, responsible for strong depolarization in response to thalamic stimulation. As shown in the example in Fig 7*D*, thalamic stimulation depolarized this 5HT3aR neuron close to threshold and occasionally elicited spikes. Fig. 7*I* shows the correlation between input resistance and EPSPs ($R^2 = 0.64$). For each neuron, evoked EPSP was normalized with the evoked EPSC in order to reveal the relationship between input resistance and changes in membrane potential without the effect of different sizes of synaptic inputs. These results demonstrate that 5HT3aR-expressing neurons receive weak but direct monosynaptic input from thalamus. Despite weak thalamocortical inputs to 5HT3aR-expressing neurons, thalamic input can depolarize a subset of 5HT3aR-expressing neurons to a similar degree as FS neurons, presumably due to their high input resistance.

Discussion

There is increasing evidence that the high diversity of GABAergic interneurons underpins the functional complexity needed for neural computation (McBain and Fisahn, 2001; Klausberger and Somogyi, 2008). Despite the promise that understanding this diversity provides, it is at present challenging to assign particular cortical functions to specific interneuron subtypes. Using a *5HT3aR-BAC*^{EGFP} transgenic mouse line combined with genetic fate mapping and analysis of neurochemical marker expression, we demonstrate that 5HT3aR-expressing neurons include the entire spectrum of CGE-derived interneurons and their associated diversity. In fact, 5HT3aR-expression labels all interneurons except the MGE-derived PV and SST populations and the progenitors that give rise to them. We discovered that in addition to the functional expression of 5HT3aRs, these cells could also be recruited robustly by cholinergic stimulation. Interestingly, we also found that some 5HT3aR neurons in TC recipient areas receive weak but potentially significant direct monosynaptic inputs from thalamus, and that a subset of 5HT3aR neurons was depolarized as strongly as FS cells by this weak input. The ability of this population to respond to serotonergic and cholinergic transmission provides a convergent means for quickly altering cortical activity through an enhancement of GABAergic synaptic transmission depending on different behavioral states.

5HT3aR-expressing neurons and cortical interneuron diversity

Interneurons in cortex comprise 15-20% of all cortical neurons in rodents (Gabbott and Somogyi, 1986; DeFelipe and Fariñas, 1992; Beaulieu, 1993; Tamamaki et al., 2003). Of this population, as much as 60% have been traditionally thought to be FS neurons (Xu et al., 2004; Butt et al., 2005; Gonchar et al., 2007). Recently, using the neuronal marker, reelin (together with SST) and VIP as CGE markers, we discovered that the contribution of cells derived from the CGE has been underestimated and in fact this population comprises as much as 30% of all cortical interneurons (Miyoshi et al., 2010). Furthermore, in this same study we also found that the peak of CGE-interneuron production was considerably later than that observed in the MGE (E16.5 and E14.5 respectively). The present finding extends our understanding of this population by demonstrating that most if not all CGE-derived interneurons express 5HT3aR, while MGE-derived PV and SST interneurons do not. Here we demonstrate that the size, breadth and diversity of this population are considerably larger than had been recognized.

This study, along with Miyoshi et al. (2010), suggests that there is a population of cortical interneurons derived from outside the MGE that does not label with any marker. This percentage seems slightly higher in this study, which could be due to the fact that *5HT3aR-BAC*^{EGFP} also labels cells outside the ganglionic eminences embryonically, most notably the POA. A majority of cortical interneurons derived from the POA as labeled by *Nkx5-1*^{Cre} genetic fate mapping have been show to lack known markers (Gelman et al., 2009). Consistent with this hypothesis, we observed EGFP-labeled interneurons with similar morphological and electrophysiological characteristics to those described by Gelman et al. (2009). Our present observation that 5HT3aR-expressing neurons constitute around 30% of cortical interneurons, adds to the growing evidence that the size and diversity of the non-FS population of interneurons have been underestimated. In fact, we find that in supragranular cortical layers, 5HT3aR interneurons are the predominant interneuron population.

Heterogenity within the 5HT3aR-expressing interneuron population

A previous study using unsupervised cluster analysis divided the 5HT3aR interneurons into two cell types: “NPY-” and “VIP-cluster”, describing them as multipolar and bipolar respectively (Vucurovic et al., 2010). Our systematic analysis of the 5HT3aR-expressing population suggests that the diversity of these neurons is much larger. We find that more than 35% of 5HT3aR-expressing neurons do not express NPY or VIP. Furthermore, we show that 5HT3aR neurons contain the entire CGE-derived population, which was previously shown to be comprised by at least nine different morphological and electrophysiological subtypes (Myoshi et al., 2010). This suggests that some caution and nuance is warranted when doing detailed analysis of the functional aspects of this population. Indeed, it is reasonable to assume that some of the heterogeneity that we see in the physiology is a reflection of functional diversity. For example, VIP or NPY expressing neurons can modulate the contraction and dilatation of nearby microvessels by releasing VIP or NPY (Cauli et al., 2004; Kocharyan et al., 2008). Thus, the activity of these neurons can potentially regulate local blood flow. Neurogliaform neurons, which presumably correspond to the LS1 subtype of 5HT3aR neurons, release GABA by volume transmission thus providing long-lasting inhibition to local circuits (Tamás et al., 2003; Oláh et al., 2009). Despite this, most 5HT3aR neurons share a developmental origin, as well as responsiveness to both serotonergic and cholinergic ascending pathways.

Functional implications of the presence of ionotropic serotonergic and acetylcholine receptors within a subpopulation of cortical interneurons

Despite the heterogeneity in the 5HT3aR-expressing population, they all share fast modulation by ionotropic serotonergic and cholinergic receptors. It is possible that their

contribution to cortical neural function is dependent on brain state and behavioral context. Perhaps 5HT3aR-expressing neurons are strongly engaged in sensory processes in specific contexts, but otherwise may provide only a weak source of inhibition within the upper layers of cortex, where they reside most prominently.

The highly biased distribution of 5HT3aR interneurons in superficial layers, especially L1, suggests that they can inhibit not only nearby neurons within superficial layers but also pyramidal neurons in infragranular layers which project their apical dendrite to superficial layers (Markram et al. 2004). Supporting this notion, pharmacological blockade of 5HT3aRs has been found to change inhibitory and excitatory tone in L5 pyramidal neurons in response to local electrical stimulation in L2/3 (Moreau et al., 2010).

5HT3aR-expressing neurons as recipients of thalamocortical input

In vivo and *in vitro* studies of thalamocortical circuits report stronger, faster and more converging projections from TC to FS neurons than to excitatory neurons (Agmon and Connors, 1991; Bruno and Simons, 2002; Swadlow, 2002; Wehr and Zador, 2003; Gabernet et al., 2005; Cruikshank et al., 2007; Hull et al., 2009). Such a bias creates strong disynaptic feedforward inhibition, resulting in spatiotemporally sharpening of incoming subcortical sensory inputs (Miller et al., 2001; Pinto et al., 2003). Low-threshold spiking (LTS) interneurons, which originate from MGE and express SST, receive sparse and weak input from thalamus compared to FS (Beierlein et al., 2003). LTS neurons are thought to be involved in feedback inhibition (Beierlein et al., 2003; Silberberg and Markram, 2007; Kapfer et al., 2007; Fanselow et al., 2008). Others have reported that “regular-spiking nonpyramidal interneurons” (RSNP), which are characterized by spike frequency adaptation, receive direct synaptic contacts from TC neurons (Porter et al., 2001). TC stimulation evoked spikes in both a subset of RSNP and FS neurons to a similar degree. The characterization of the RSNP cells receiving TC input in the Porter et al. (2001) study was insufficient to definitely determine the subtypes, but it is highly likely that at least some of them correspond to 5HT3aR cells. Under our experimental conditions, about 65% of 5HT3aR-expressing neurons in deep layer 3 and layer 4 received weak but monosynaptic inputs from TC stimulation. Despite the small TC synaptic current recorded in 5HT3aR-expressing neurons, TC stimulation strongly depolarized a subset of these TC recipients similar to FS neurons. This can be explained, in part, as a result of their high input resistance.

Our finding of strong depolarization of a subset of 5HT3aR neurons in response to TC stimulation raises the possibility that these 5HT3aR neurons can contribute to feedforward inhibition in TC circuits. The dynamics of feedforward inhibition by 5HT3aR neurons, however, may differ compared to that by FS neurons. On the other hand some of the TC recipient 5HT3aR neurons could predominantly inhibit other interneurons, including FS neurons, and thus indirectly relieve excitatory neurons from feedforward inhibition. Anatomical evidence supports that a majority of FS neurons in S1 cortex receive synaptic contacts from VIP neurons (Dávid et al., 2007).

Serotonin and ACh may sensitize 5HT3aR neurons and increase their responsiveness to TC input, thus making feedforward inhibition of TC inputs or the relieve of excitatory neurons from feedforward inhibition dependent on behavioral state. Understanding the mechanisms by which serotonergic and/or cholinergic afferents on these TC-recipient 5HT3aR neurons modulate sensory input, will no doubt add considerably to our understanding of cortical circuitry.

In future studies it will be important to investigate the synaptic connectivity among FS, pyramidal and 5HT3aR neurons, to understand dynamics of cortical circuits and how these

synaptic properties are modulated by serotonin and acetylcholine. Extending this line of studies to *in vivo* preparations will be important in order to understand how 5HT3aR neurons are engaged in network dynamics in the context of sensory processing in cortex during different brain states.

Acknowledgments

We thank members of the Rudy and Fishell labs for their advice and support. SL is supported by the Patterson trust fellowship. J.H-L is supported by a long-term EMBO fellowship and the Swedish Society for Medical Research (SSMF). This research was supported by National Institutes of Health Grants NS30989 and NS045217 to BR, and R01MS226557 and R01NS039007 to GF.

References

Agmon A, Connors BW. Thalamocortical responses of mouse somatosensory (barrel) cortex in vitro. Neuroscience. 1991; 41:365–79. [PubMed: 1870696]

Anderson SA, Qiu M, Bulfone A, Eisenstat DD, Meneses J, Pedersen R, Rubenstein JL. Mutations of the homeobox genes Dlx-1 and Dlx-2 disrupt the striatal subventricular zone and differentiation of late born striatal neurons. Neuron. 1997a; 19:27–37. [PubMed: 9247261]

Anderson SA, Eisenstat DD, Shi L, Rubenstein JL. Interneuron migration from basal forebrain to neocortex: dependence on Dlx genes. Science. 1997b; 278:474–6. [PubMed: 9334308]

Ascoli GA, et al. Petilla Interneuron Nomenclature Group. Petilla terminology: nomenclature of features of GABAergic interneurons of the cerebral cortex. Nat Rev Neurosci. 2008; 9:557–68. [PubMed: 18568015]

Barnes NM, Sharp T. A review of central 5-HT receptors and their function. Neuropharmacology. 1999; 38:1083–152. [PubMed: 10462127]

Battiste J, Helms AW, Kim EJ, Savage TK, Lagace DC, Mandyam CD, Eisch AJ, Miyoshi G, Johnson JE. Ascl1 defines sequentially generated lineage-restricted neuronal and oligodendrocyte precursor cells in the spinal cord. Development. 2007; 134:285–93. [PubMed: 17166924]

Beaulieu C. Numerical data on neocortical neurons in adult rat, with special reference to the GABA population. Brain Res. 1993; 609:284–92. [PubMed: 8508310]

Beaulieu C, Somogyi P. Enrichment of cholinergic synaptic terminals on GABAergic neurons and coexistence of immunoreactive GABA and choline acetyltransferase in the same synaptic terminals in the striate cortex of the cat. J Comp Neurol. 1991; 304:666–80. [PubMed: 2013651]

Beierlein M, Gibson JR, Connors BW. Two dynamically distinct inhibitory networks in layer 4 of the neocortex. J Neurophysiol. 2003; 90:2987–3000. [PubMed: 12815025]

Bhat RV, Axt KJ, Fosnaugh JS, Smith KJ, Johnson KA, Hill DE, Kinzler KW, Baraban JM. Expression of the APC tumor suppressor protein in oligodendroglia. Glia. 1996; 17:169–174. [PubMed: 8776583]

Britanova O, de Juan Romero C, Cheung A, Kwan KY, Schwark M, Gyorgy A, Vogel T, Akopov S, Mitkovski M, Agoston D, Sestan N, Molnár Z, Tarabykin V. Satb2 is a postmitotic determinant for upper-layer neuron specification in the neocortex. Neuron. 2008; 57:378–92. [PubMed: 18255031]

Bruno RM, Simons DJ. Feedforward mechanisms of excitatory and inhibitory cortical receptive fields. J Neurosci. 2002; 22:10966–75. [PubMed: 12486192]

Butt SJ, Fuccillo M, Nery S, Noctor S, Kriegstein A, Corbin JG, Fishell G. The temporal and spatial origins of cortical interneurons predict their physiological subtype. Neuron. 2005; 48:591–604. [PubMed: 16301176]

Buzsáki G, Geisler C, Henze DA, Wang XJ. Interneuron Diversity series: Circuit complexity and axon wiring economy of cortical interneurons. Trends Neurosci. 2004; 27:186–93. [PubMed: 15046877]

Caputi A, Rozov A, Blatow M, Monyer H. Two calretinin-positive GABAergic cell types in layer 2/3 of the mouse neocortex provide different forms of inhibition. Cereb Cortex. 2009; 19:1345–59. [PubMed: 18842664]

Cauli B, Audinat E, Lambolez B, Angulo MC, Ropert N, Tsuzuki K, Hestrin S, Rossier J. Molecular and physiological diversity of cortical nonpyramidal cells. J Neurosci. 1997; 17:3894–906. [PubMed: 9133407]

Cauli B, Porter JT, Tsuzuki K, Lambolez B, Rossier J, Quenet B, Audinat E. Classification of fusiform neocortical interneurons based on unsupervised clustering. Proc Natl Acad Sci USA. 2000; 97:6144–9. [PubMed: 10823957]

Cauli B, Tong XK, Rancillac A, Serluca N, Lambolez B, Rossier J, Hamel E. Cortical GABA interneurons in neurovascular coupling: relays for subcortical vasoactive pathways. J Neurosci. 2004; 24(41):8940–9. [PubMed: 15483113]

Chameau P, Inta D, Vitalis T, Monyer H, Wadman WJ, van Hooft JA. The N-terminal region of reelin regulates postnatal dendritic maturation of cortical pyramidal neurons. Proc Natl Acad Sci USA. 2009; 106:7227–32. [PubMed: 19366679]

Chameau P, van Hooft JA. Serotonin 5-HT(3) receptors in the central nervous system. Cell Tissue Res. 2006; 326:573–81. [PubMed: 16826372]

Chattopadhyaya B, Di Cristo G, Higashiyama H, Knott GW, Kuhlman SJ, Welker E, Huang ZJ. Experience and activity-dependent maturation of perisomatic GABAergic innervation in primary visual cortex during a postnatal critical period. J Neurosci. 2004; 24:9598–611. [PubMed: 15509747]

Chu Z, Galarreta M, Hestrin S. Synaptic interactions of late-spiking neocortical neurons in layer 1. J Neurosci. 2003; 23:96–102. [PubMed: 12514205]

Cobos I, Long JE, Thwin MT, Rubenstein JL. Cellular patterns of transcription factor expression in developing cortical interneurons. Cereb Cortex Suppl. 2006; 1:i82–8.

Cruikshank SJ, Lewis TJ, Connors BW. Synaptic basis for intense thalamocortical activation of feedforward inhibitory cells in neocortex. Nat Neurosci. 2007; 10:462–8. [PubMed: 17334362]

Cruikshank SJ, Urabe H, Nurmikko AV, Connors BW. Pathway-specific feedforward circuits between thalamus and neocortex revealed by selective optical stimulation of axons. Neuron. 2010; 65:230–45. [PubMed: 20152129]

Dávid C, Schleicher A, Zuschratter W, Staiger JF. The innervation of parvalbumin-containing interneurons by VIP-immunopositive interneurons in the primary somatosensory cortex of the adult rat. Eur J Neurosci. 2007; 25:2329–40. [PubMed: 17445231]

DeFelipe J, Fariñas I. The pyramidal neuron of the cerebral cortex: morphological and chemical characteristics of the synaptic inputs. Prog Neurobiol. 1992; 39:563–607. [PubMed: 1410442]

Dumitriu D, Cossart R, Huang J, Yuste R. Correlation between axonal morphologies and synaptic input kinetics of interneurons from mouse visual cortex. Cereb Cortex. 2007; 17:81–91. [PubMed: 16467567]

Fanselow EE, Richardson KA, Connors BW. Selective, state-dependent activation of somatostatin-expressing inhibitory interneurons in mouse neocortex. J Neurophysiol. 2008; 100:2640–52. [PubMed: 18799598]

Férézou I, Cauli B, Hill EL, Rossier J, Hamel E, Lambolez B. 5-HT3 receptors mediate serotonergic fast synaptic excitation of neocortical vasoactive intestinal peptide/cholecystokinin interneurons. J Neurosci. 2002; 22:7389–97. [PubMed: 12196560]

Freund TF. Interneuron Diversity series: Rhythm and mood in perisomatic inhibition. Trends Neurosci. 2003; 26:489–95. [PubMed: 12948660]

Freund TF, Buzsáki G. Interneurons of the hippocampus. Hippocampus. 1996; 6:347–470. [PubMed: 8915675]

Gabbott PL, Somogyi P. Quantitative distribution of GABA-immunoreactive neurons in the visual cortex (area 17) of the cat. Exp Brain Res. 1986; 61:323–31. [PubMed: 3005016]

Gabernet L, Jadhav SP, Feldman DE, Carandini M, Scanziani M. Somatosensory integration controlled by dynamic thalamocortical feed-forward inhibition. Neuron. 2005; 48:315–27. [PubMed: 16242411]

Galarreta M, Erdélyi F, Szabó G, Hestrin S. Electrical coupling among irregular-spiking GABAergic interneurons expressing cannabinoid receptors. J Neurosci. 2004; 24:9770–8. [PubMed: 15525762]

Gelman DM, Martini FJ, Nóbrega-Pereira S, Pierani A, Kessaris N, Marín O. The embryonic preoptic area is a novel source of cortical GABAergic interneurons. J Neurosci. 2009; 29:9380–9. [PubMed: 19625528]

Gonchar Y, Wang Q, Burkhalter A. Multiple distinct subtypes of GABAergic neurons in mouse visual cortex identified by triple immunostaining. Front Neuroanat. 2007; 1:3. [PubMed: 18958197]

Hull C, Isaacson JS, Scanziani M. Postsynaptic mechanisms govern the differential excitation of cortical neurons by thalamic inputs. J Neurosci. 2009; 29:9127–36. [PubMed: 19605650]

Inta D, Alfonso J, von Engelhardt J, Kreuzberg MM, Meyer AH, van Hooft JA, Monyer H. Neurogenesis and widespread forebrain migration of distinct GABAergic neurons from the postnatal subventricular zone. Proc Natl Acad Sci USA. 2008; 105:20994–9. [PubMed: 19095802]

Kapfer C, Glickfeld LL, Atallah BV, Scanziani M. Supralinear increase of recurrent inhibition during sparse activity in the somatosensory cortex. Nat Neurosci. 2007; 10:743–53. [PubMed: 17515899]

Karagiannis A, Gallopin T, Dávid C, Battaglia D, Geoffroy H, Rossier J, Hillman EM, Staiger JF, Cauli B. Classification of NPY-expressing neocortical interneurons. J Neurosci. 2009; 29(11): 3642–59. [PubMed: 19295167]

Kawaguchi Y. Physiological subgroups of nonpyramidal cells with specific morphological characteristics in layer II/III of rat frontal cortex. J Neurosci. 1995; 15(4):2638–55. [PubMed: 7722619]

Kawaguchi Y, Kubota Y. Physiological and morphological identification of somatostatin- or vasoactive intestinal polypeptide-containing cells among GABAergic cell subtypes in rat frontal cortex. J Neurosci. 1996; 16:2701–15. [PubMed: 8786446]

Kawaguchi Y, Kubota Y. GABAergic cell subtypes and their synaptic connections in rat frontal cortex. Cereb Cortex. 1997; 7:476–86. [PubMed: 9276173]

Klausberger T, Somogyi P. Neuronal diversity and temporal dynamics: the unity of hippocampal circuit operations. Science. 2008; 321:53–7. [PubMed: 18599766]

Kocharyan A, Fernandes P, Tong XK, Vaucher E, Hamel E. Specific subtypes of cortical GABA interneurons contribute to the neurovascular coupling response to basal forebrain stimulation. J Cereb Blood Flow Metab. 2008; 28:221–31. [PubMed: 17895909]

Kruglikov I, Rudy B. Perisomatic GABA release and thalamocortical integration onto neocortical excitatory cells are regulated by neuromodulators. Neuron. 2008; 58:911–24. [PubMed: 18579081]

Lewis DA, Hashimoto T. Deciphering the disease process of schizophrenia: the contribution of cortical GABA neurons. Int Rev Neurobiol. 2007; 78:109–31. [PubMed: 17349859]

Lu QR, Yuk D, Alberta JA, Zhu Z, Pawlitzky I, Chan J, McMahon AP, Stiles CD, Rowitch DH. Sonic hedgehog--regulated oligodendrocyte lineage genes encoding bHLH proteins in the mammalian central nervous system. Neuron. 2000; 25:317–29. [PubMed: 10719888]

Luche H, Weber O, Nageswara Rao T, Blum C, Fehling HJ. Faithful activation of an extra-bright red fluorescent protein in “knock-in” Cre-reporter mice ideally suited for lineage tracing studies. Eur J Immunol. 2007; 37:43–53. [PubMed: 17171761]

Markram H, Toledo-Rodriguez M, Wang Y, Gupta A, Silberberg G, Wu C. Interneurons of the neocortical inhibitory system. Nat Rev Neurosci. 2004; 5:793–807. [PubMed: 15378039]

McBain CJ, Fisahn A. Interneurons unbound. Nat Rev Neurosci. 2001; 2:11–23. [PubMed: 11253355]

Miller KD, Pinto DJ, Simons DJ. Processing in layer 4 of the neocortical circuit: new insights from visual and somatosensory cortex. Curr Opin Neurobiol. 2001; 11:488–97. [PubMed: 11502397]

Miyoshi G, Butt SJ, Takebayashi H, Fishell G. Physiologically distinct temporal cohorts of cortical interneurons arise from telencephalic Olig2-expressing precursors. J Neurosci. 2007; 27(29):7786–98. [PubMed: 17634372]

Miyoshi G, Hjerling-Leffler J, Karayannis T, Sousa VH, Butt SJ, Battiste J, Johnson JE, Machold RP, Fishell G. Genetic fate mapping reveals that the caudal ganglionic eminence produces a large and diverse population of superficial cortical interneurons. J Neurosci. 2010; 30(5):1582–94. [PubMed: 20130169]

Morales M, Bloom FE. The 5-HT3 receptor is present in different subpopulations of GABAergic neurons in the rat telencephalon. J Neurosci. 1997; 17:3157–67. [PubMed: 9096150]

Moreau AW, Amar M, Le Roux N, Morel N, Fossier P. Serotoninergic fine-tuning of the excitation-inhibition balance in rat visual cortical networks. Cereb Cortex. 2010; 20:456–67. [PubMed: 19520765]

Nery S, Fishell G, Corbin JG. The caudal ganglionic eminence is a source of distinct cortical and subcortical cell populations. Nat Neurosci. 2002; 5:1279–87. [PubMed: 12411960]

Oláh S, Füle M, Komlósi G, Varga C, Báldi R, Barzó P, Tamás G. Regulation of cortical microcircuits by unitary GABA-mediated volume transmission. Nature. 2009; 461(7268):1278–81. [PubMed: 19865171]

Oláh S, Komlósi G, Szabadics J, Varga C, Tóth E, Barzó P, Tamás G. Output of neurogliaform cells to various neuron types in the human and rat cerebral cortex. Front Neural Circuits. 2007; 1:4. [PubMed: 18946546]

Oliva AA Jr, Jiang M, Lam T, Smith KL, Swann JW. Novel hippocampal interneuronal subtypes identified using transgenic mice that express green fluorescent protein in GABAergic interneurons. J Neurosci. 2000; 20:3354–68. [PubMed: 10777798]

Pesold C, Liu WS, Guidotti A, Costa E, Caruncho HJ. Cortical bitufted, horizontal, and Martinotti cells preferentially express and secrete reelin into perineuronal nets, nonsynaptically modulating gene expression. Proc Natl Acad Sci USA. 1999; 96:3217–22. [PubMed: 10077664]

Pinto DJ, Hartings JA, Brumberg JC, Simons DJ. Cortical damping: analysis of thalamocortical response transformations in rodent barrel cortex. Cereb Cortex. 2003; 13:33–44. [PubMed: 12466213]

Porter JT, Cauli B, Staiger JF, Lambolez B, Rossier J, Audinat E. Properties of bipolar VIPergic interneurons and their excitation by pyramidal neurons in the rat neocortex. Eur J Neurosci. 1998; 10:3617–28. [PubMed: 9875341]

Porter JT, Johnson CK, Agmon A. Diverse types of interneurons generate thalamus-evoked feedforward inhibition in the mouse barrel cortex. J Neurosci. 2001; 21(8):2699–710. [PubMed: 11306623]

Rozov A, Jerecic J, Sakmann B, Burnashev N. AMPA receptor channels with long-lasting desensitization in bipolar interneurons contribute to synaptic depression in a novel feedback circuit in layer 2/3 of rat neocortex. J Neurosci. 2001; 21:8062–71. [PubMed: 11588179]

Silberberg G, Markram H. Disynaptic inhibition between neocortical pyramidal cells mediated by Martinotti cells. Neuron. 2007; 53:735–46. [PubMed: 17329212]

Smiley JF, Goldman-Rakic PS. Serotonergic axons in monkey prefrontal cerebral cortex synapse predominantly on interneurons as demonstrated by serial section electron microscopy. J Comp Neurol. 1996; 367:431–43. [PubMed: 8698902]

Sousa VH, Miyoshi G, Hjerling-Leffler J, Karayannis T, Fishell G. Characterization of Nkx6-2-derived neocortical interneuron lineages. Cereb Cortex. 2009; 19:i1–i10. [PubMed: 19363146]

Swadlow HA. Thalamocortical control of feed-forward inhibition in awake somatosensory ‘barrel’ cortex. Philos Trans R Soc Lond B Biol Sci. 2002; 357:1717–27. [PubMed: 12626006]

Swadlow HA, Gusev AG. The influence of single VB thalamocortical impulses on barrel columns of rabbit somatosensory cortex. J Neurophysiol. 2000; 83:2802–13. [PubMed: 10805678]

Tamamaki N, Yanagawa Y, Tomioka R, Miyazaki J, Obata K, Kaneko T. Green fluorescent protein expression and colocalization with calretinin, parvalbumin, and somatostatin in the GAD67-GFP knock-in mouse. J Comp Neurol. 2003; 467:60–79. [PubMed: 14574680]

Tamás G, Lorincz A, Simon A, Szabadics J. Identified sources and targets of slow inhibition in the neocortex. Science. 2003; 299:1902–5. [PubMed: 12649485]

Tricoire L, Pelkey KA, Daw MI, Sousa VH, Miyoshi G, Jeffries B, Cauli B, Fishell G, McBain CJ. Common origins of hippocampal Ivy and nitric oxide synthase expressing neurogliaform cells. J Neurosci. 2010; 30:2165–76. [PubMed: 20147544]

Varga V, Losonczy A, Zemelman BV, Borhegyi Z, Nyiri G, Domonkos A, Hangya B, Holderith N, Magee JC, Freund TF. Fast synaptic subcortical control of hippocampal circuits. Science. 2009; 326:449–53. [PubMed: 19833972]

Vucurovic K, Gallopin T, Ferezou I, Rancillac A, Chameau P, van Hooft JA, Geoffroy H, Monyer H, Rossier J, Vitalis T. Serotonin 3A Receptor Subtype as an Early and Protracted Marker of Cortical Interneuron Subpopulations. Cereb Cortex. Jan 18.2010 [Epub ahead of print].

Wainer BH, Bolam JP, Freund TF, Henderson Z, Totterdell S, Smith AD. Cholinergic synapses in the rat brain: a correlated light and electron microscopic immunohistochemical study employing a monoclonal antibody against choline acetyltransferase. Brain Res. 1984; 308:69–76. [PubMed: 6478204]

Wehr M, Zador AM. Balanced inhibition underlies tuning and sharpens spike timing in auditory cortex. Nature. 2003; 426:442–6. [PubMed: 14647382]

Wichterle H, Garcia-Verdugo JM, Herrera DG, Alvarez-Buylla A. Young neurons from medial ganglionic eminence disperse in adult and embryonic brain. Nat Neurosci. 1999; 2:461–6. [PubMed: 10321251]

Wichterle H, Turnbull DH, Nery S, Fishell G, Alvarez-Buylla A. In utero fate mapping reveals distinct migratory pathways and fates of neurons born in the mammalian basal forebrain. Development. 2001; 128:3759–71. [PubMed: 11585802]

Wilent WB, Contreras D. Dynamics of excitation and inhibition underlying stimulus selectivity in rat somatosensory cortex. Nat Neurosci. 2005; 8:1364–70. [PubMed: 16158064]

Wonders CP, Anderson SA. The origin and specification of cortical interneurons. Nat Rev Neurosci. 2006:687–96. [PubMed: 16883309]

Xu Q, Cobos I, De La Cruz E, Rubenstein JL, Anderson SA. Origins of cortical interneuron subtypes. J Neurosci. 2004; 24:2612–22. [PubMed: 15028753]

Xu Q, Tam M, Anderson SA. Fate mapping Nkx2.1-lineage cells in the mouse telencephalon. J Comp Neurol. 2008; 506:16–29. [PubMed: 17990269]

Zhou Q, Anderson DJ. The bHLH transcription factors OLIG2 and OLIG1 couple neuronal and glial subtype specification. Cell. 2002; 109:61–73. [PubMed: 11955447]

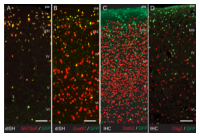

Fig 1.

5HT3aR-BAC^{EGFP} cells of the somatosensory cortex are 5HT3aR-expressing GABAergic interneurons. ***A-B***, Double *in situ* hybridization for *5HT3aR* and *EGFP/GAD67*. ***A***, Double *in situ* for *5HT3aR* and *EGFP* show complete overlap in the adult somatosensory cortex. ***B***, All *5HT3aR* positive cells are also *GAD67* positive. ***C-D***, immunohistochemistry for GFP and Satb2/Olig2. ***C***, No overlap with pyramidal cell markers as Satb2 confirms the interneuron identity. ***D***, No EGFP-positive cells express oligodendrocyte marker Olig2. Scale bars = 100 μm. dISH, double in situ hybridization; IHC, immunohistochemistry.

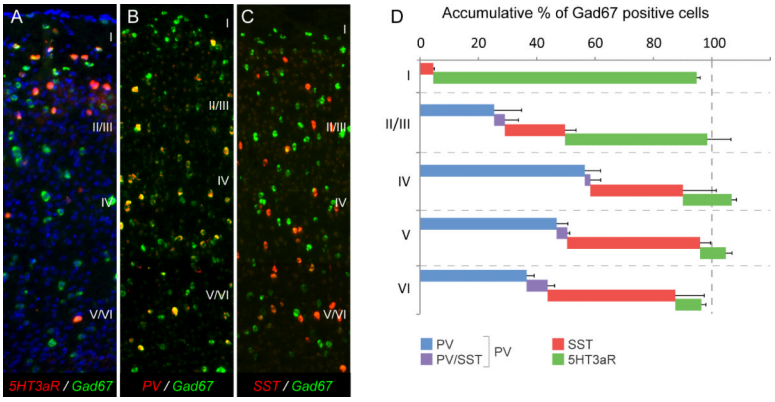

Fig 2.

5HT3aR-expressing cells are the third major group of cortical interneurons. ***A-C***, Double *in situ* hybridization (dISH) for the three markers *PV*, *SST* and *5HT3aR* with pan-GABAergic marker *Gad67*. ***D***, Cumulative graph showing the percentage of *Gad67* cells expressing each marker. Note that 100 ± 5% of interneurons of all layers can be accounted for using these three markers and that 5HT3aR-expressing neurons predominantly occupy superficial layers. Notably we observed some overlap in the *in situ* signal between *SST* and *PV* even though this cannot be seen at the protein level.

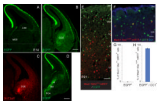

Fig 3.

A-D, *5HT3aR-BAC*^{EGFP} mice have labeled neurons in the CGE (as well as more ventral structures) but not the LGE or MGE. This EGFP expression reflects true *5HT3aR* mRNA expression as shown by ISH for *5HT3aR* (***C***). ***E-H***, Genetic fate mapping confirms that 5HT3aR-expressing cells in mature cortex are CGE derived. We used *Nkx2.1-BAC*^{Cre} and *Mash1-BAC*^{CreER}, mouse lines in combination with the R26R^{tdRFP}-reporter crossed onto the *5HT3aR-BAC*^{EGFP} to label cells embryonically and follow their fate into the mature cortex. ***G,H***, The complete lack of *Nkx2.1-BAC*^{Cre}*;R26R*^{tdRFP} and *5HT3aR-BAC*^{EGFP} overlap shows that the cells are not of MGE origin while the almost complete overlap with *Mash1-BAC*^{CreER};R26R^{tdRFP} labeled interneurons confirms the CGE origin. CC1 was used as a marker to exclude RFP-expressing oligodendrocytes from quantization (***H***). Scale bars: *B,D* = 250 μm; *E* = 100 μm; *F* = 50 μm.

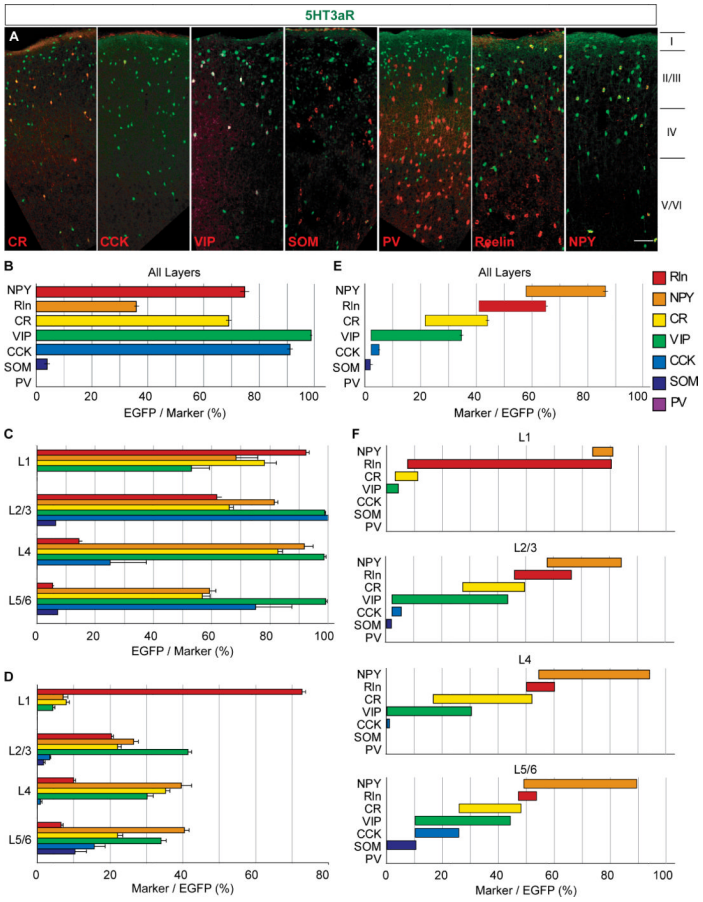

Fig 4.

Neurochemical marker expression profiles of 5HT3aR-expressing cortical interneurons. ***A***, Immunofluorescent histochemistry show the relationship of seven neuronal markers (CR, CCK, VIP, SST, PV, Rln, and NPY) and 5HT3aR-positive neurons in somatosensory cortex (p = 21 to 25) of *5HT3aR-BAC*^{EGFP} mice (n = 3). ***B***, the percentage of specific neuronal markers that is also positive for EGFP across all layers (EGFP/marker). ***C***, same as in *B* but analyzed per layer. ***D***, The percentage of 5HT3aR-expressing neurons expressing specific neuronal markers per individual layers (marker/EGFP). ***E***, The proportion of 5HT3aR-expressing neurons expressing specific neuronal markers across all layers (marker/EGFP), individual bars are displaced to illustrate the overlap due to co-localization of markers. ***F***, Same as *E* but analyzed per layer. Note that more than 85% of 5HT3aR-expressing neurons were found to express at least one of the 7 neuronal markers. Rln, Reelin; NPY, Neuropeptide Y; CR, Calretinin; VIP, Vasoactive intestinal peptide; CCK, Cholecystokinin; SOM, Somatostatin; PV, Parvalbumin. Scale bar = 100 μm.

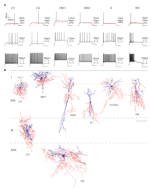

Fig 5.

Intrinsic electrophysiological properties and morphologies of 5HT3aR-expressing cortical interneurons. ***A***, Representative traces of voltage responses to 500 ms step current injection in current clamp whole-cell configuration of 6 major subtypes of 5HT3aR interneurons. ***B***, Examples of morphologies of different subtypes reconstructed using neurolucida tracing. Dendrite and soma are shown in blue and axon in red. LS1, late spiking 1; LS2, late spiking 2; bNA1, burst non-adapting 1; bNA2, burst nonadapting 2; IS, irregular spiking; fAD, fast adapting; POA, pre-optic area. Scale bar = 100 μm.

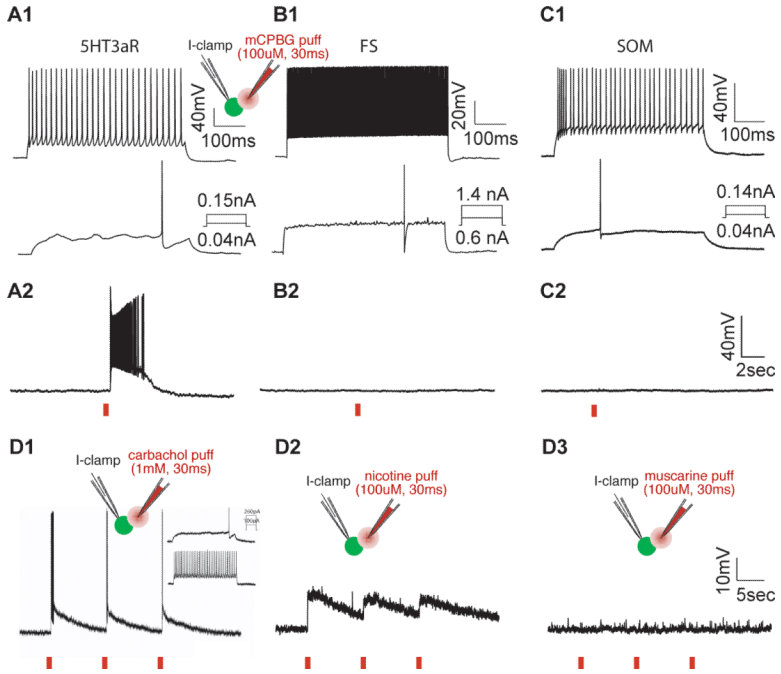

Fig 6.

Functional expression of 5HT3aRs and nAChRs in 5HT3aR-expressing interneurons. Intrinsic firing patterns to step current injections recorded from three different types of cortical interneurons from *5HT3aR-BAC*^{EGFP} (***A1***), B13 (***B1***) and GIN (***C1***) transgenic mice. Application of a 5HT3aR selective agonist (mCPBG, 100uM, 30ms puffing) causes strong depolarization and evokes a burst of spikes in 5HT3aR cells (***A2***) but not in FS (***B2***) or SST-expressing cells (***C2***). ***D***, Functional expression of nACh receptors in EGFP positive neurons of *5HT3aR-BAC*^{EGFP} mouse. ***D1***, Carbachol application (1mM) strongly depolarizes and evokes burst of spikes in a 5HT3aR neuron recorded in whole cell configuration in current clamp (30ms puff indicated by red line below). Inset show intrinsic firing pattern of recorded cell to step current injections. ***D2***, Functional expression of nicotinic ACh receptors in EGFP positive neurons of *5HT3aRBAC*^{EGFP} mouse. Nicotine puffing (100uM for 30ms) depolarizes the 5HT3aR neuron (***D2***) but muscarine application (***D3***) to the same neuron did not change membrane potential indicating 5HT3aR interneurons express nicotinic AChRs. Insets in *A1* and *D1-D3* show schematics of the recording configuration.

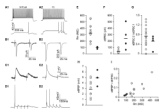

Fig 7.

Monosynaptic thalamocortical input to 5HT3aR-expressing neurons. ***A***, Voltage responses of 5HT3aR (**A1**) and FS (**A2**) neurons to 500 ms step current injection. ***B***, Weak monosynaptic TC input to 5HT3aR-expressing neurons. Stimulation of TC afferents evokes smaller EPSCs onto a 5HT3aR (***B1***) as compared to a FS neurons (***B2***) recorded in the whole cell voltage-clamp configuration (note difference in scale). ***C***, TC stimulation depolarized a 5HT3aR neuron (***C1***) in a similar degree to a FS neuron (***C2***). Under current-clamp configuration (Vm = -65 mV), voltage responses to TC stimulation were recorded from the same example 5HT3aR and FS neurons shown in *B1* and *B2*, respectively. ***D***, TC stimulation can elicit spikes in a 5HT3aR neuron. Increased intensity of TC stimulation evoked spikes in a 5HT3aR (***D1***) and a FS neuron (***D2***). Summary data comparing input resistance (***E***), evoked EPSC (***F***), synaptic depression (***G***), and evoked EPSP (***H***) of 5HT3aR and FS neurons to 20Hz TC stimulation. Green and red open circles indicate 5HT3aR and FS neurons, respectively. Bars indicate mean values. ***I***, Relationship between input resistance (Rm) and evoked membrane depolarization (eEPSP) normalized with eEPSC to TC stimulation.

Table 1

Quantification of electrophysiological properties of 5HT3aR-expressing neurons in layer 2/3 (n = 80).

	LS1	LS2	bNA1	bNA2	IS	dNFS3	fAD
RMP (mV)	-61.2 ± 5.8	-60.5 ± 7.0	-63 ± 4.3	-60.2 ± 5.7	-58.4 ± 5.9	-65 ± 6.3	-56.9 ± 7.0
Rm(MΩ)	329 ± 89	285 ± 101	332 ±124	369 ±143	406 ± 132	631 ± 310	459 ± 179
τm (ms)	17.3 ± 6.5	19.3 ± 5.8	17.5 ± 8.5	19.4 ± 8.3	20.1 ± 7.1	27.7 ± 12.3	26.4 ± 9.7
Spike thresh. (mV)	-38.2 ± 5.4	-36.9 ± 5.1	-35.5 ± 4.5	-36.1 ± 3.8	-39.8 ± 6.3	-42.2 ± 6.1	-38.3 ± 4.9
Spike width (ms)	1.4 ± 0.5	1.4 ± 0.4	1.4 ±0.6	1.4 ±0.4	1.2 ± 0.4	1.3 ± 0.3	1.1 ± 0.3
AHP amp (mV)	-19.3 ± 5.2	-18.2 ± 3.9	-16.1 ± 5.1	-14.4 ± 4.6	-13.0 ± 0.4	-15.3 ± 3.3	-12.2 ± 3.4
tAHP (ms)	23.1 ± 4.8	24.8 ± 7.9	50.3 ± 11.9	24.9 ± 8.5	14.2 ± 5.2	14.1 ± 9.8	18.1 ± 9.9
Delay to spike (ms)	376.3 ± 79.8	224.8 ± 130.1	70.3 ± 21.4	75.4 ± 41.4	259.5 ± 120.5	14.1 ± 9.8	18.1 ± 9.9
Max Freq. (Hz)	79.3 ± 30.1	59.2 ± 18.4	52.6 ± 14.9	61.5 ± 28.4	84.9 ± 16.5	81.3 ± 21.4	85.7 ± 21.5
Adaptation (%)	51.3 ± 14.5	53.9 ± 16.3	63.7 ± 18.2	59.4 ± 21.4	41.5 ± 11.6	36.3 ± 9.8	N/A

See materials and Methods for an explanation of the parameters.